JOURNAL OF CATALYSIS 129, 257–268 (1991)

Electron Microdiffraction Study of Pt–Sn–Alumina Reforming Catalysts

RAM SRINIVASAN,* LARRY A. RICE,† AND BURTRON H. DAVIS*

*Center for Applied Energy Research, University of Kentucky, 3572 Iron Works Pike, Lexington, Kentucky 40511; and †Department of Materials Science and Engineering, University of Kentucky, Lexington, Kentucky 40506

Received September 12, 1990; revised December 19, 1990

An electron microdiffraction technique was employed to identify crystal structures developed in two Pt–Sn–alumina catalysts. One catalyst was prepared by coprecipitating Sn and Al and then impregnating the calcined material with hexachloroplatinic acid to give a Pt : Sn = 1 : 3 atomic ratio. The second catalyst was prepared by coimpregnating Degussa Al_2O_3 with an acetone solution of H_2PtCl_6 and $SnCl_4$ to provide a Pt : Sn ratio of 1 : 3. Pt–Sn alloy was not detected by X-ray diffraction for coprecipitated catalyst although evidence for Pt–Sn alloy was found for the coimpregnated catalyst. However, electron microdiffraction studies clearly showed evidence for Pt : Sn = 1 : 1 (hcp) alloy phase in both the catalysts. Evidence for the presence of minor amounts of Pt : Sn = 1 : 2 (fcc) phase was also found for the coprecipitated catalyst. EDX analysis of selected particles show that the dominant alloy is Pt : Sn = 1 : 1 for the coimpregnated catalyst. However, for the coprecipitated catalyst, most of the Pt appear as the metal, and not an alloy. Much of the tin is not detected by EDX for the coprecipitated catalyst.

INTRODUCTION

Reforming catalysts such as Pt–Re or Pt–Sn are assuming increasingly important roles in naphtha reforming processes. These bimetallic catalysts are known for their resistance to aging. Pt–Re–alumina was introduced by Chevron (*1*). This bimetallic catalyst showed high selectivity for aromatic products; it was quite stable, exhibited longer catalytic life, and permitted operations at high temperatures. Recently, the Pt–Sn bimetallic combination has attracted much attention since it is a potential candidate for commercial applications, especially for low-pressure operation and in processes employing continuous regeneration. Better understanding of the structures of the metallic components in these catalysts is needed. Both direct and indirect methods of analyzing these catalysts have been employed. The state of tin in these catalysts has become a matter of intense research.

The reasons for the superior catalytic properties of these bimetallic catalysts remain to be explained even after 30 years of active research in this area. Many of the explanations for the superior properties of the bimetallic catalysts are based on a structural point of view. The bimetallic components are believed to form alloys which have better catalytic properties. For example, alloy formation could influence the *d*-band electron concentration, thereby controlling selectivity and activity. On the other hand, the superior activity and selectivity may be the result of dispersion of the active Pt component and the stabilization of the dispersed phase by the second component (*2*). Thus, much effort has been expended to define the extent to which metallic alloys are formed (for example, *3–15*). Subsequently, various experimental techniques were devised to study the structures of the alloys.

Temperature-programmed reduction (TPR), one of the indirect analysis methods, yielded data that suggested that Sn was not reduced to zero-valent state (*6, 16*). Lieske and Volter (*17*) reported, based on the results obtained from TPR studies, that a mi-

0021-9517/91 $3.00

nor part of the tin is reduced to the metal, which combined with Pt to form "alloy clusters" and the major portion of the tin is reduced to Sn (II) state. They also reported that the amount of alloyed tin increases with increasing tin content.

X-ray photoelectron spectroscopy (XPS) studies revealed that the tin is present only in an oxidized state (*8, 14*); however, other XPS studies were consistent with alloy formation (*18, 19*). Re was also not found in the metallic state in Pt–Re bimetallic catalysts (*7, 20*). These XPS data stood in conflict with the extensive experimental data that strongly suggested the alloy formation.

Mössbauer spectroscopy, another direct analysis method, showed evidence for Pt–Sn alloy formation (*4, 5, 21, 22*). However, the catalysts used for these studies had higher metal loadings, and even then the spectrum was so complex that there was uncertainty in showing the presence of Sn metal. Kuznetsov *et al.* (*15*) reported that Pt–Sn–α-Al_2O_3 catalysts have highly dispersed products such as Sn(IV), Sn(II), and Sn(O). According to these authors (*15*), Pt forms nearly all possible alloys with tin.

At least five Pt–Sn alloys exist; crystallographic information of these alloys are given in Table 1 (*23*). The Pt–Sn alloy exhibits "hcp" structure, $PtSn_2$ is "fcc," Pt–Sn_4 is orthorhombic, and Pt_3Sn is fcc (Cu_3Au type). It is therefore possible to identify and quantify Pt/Sn alloy phases of these bimetallic catalysts from crystallographic data. Ushakov and Moroz (*24*), using *in situ* XRD data, concluded that only half of the Pt on the alumina support was reduced in H_2 at 500°C; the other half was ionic Pt bonded to the support or a highly dispersed state of zero-valent Pt. In another *in situ* XRD study (*25*), it was shown that Pt–Sn alloy (hcp) was formed for 5 wt% or 0.6 wt% Pt–Sn–alumina catalysts following reduction at 500°C for 8 h; no other Pt–Sn alloy was found. The Pt–Sn (hcp) alloy could be reoxidized and then regenerated by subsequent reduction.

In the present investigation, an electron microdiffraction technique is employed in another attempt to identify alloy phases in Pt–Sn bimetallic catalysts.

EXPERIMENTAL PROCEDURES

A. Catalysts

Two Pt–Sn catalysts were used in the present investigation. CAT-A was prepared by impregnating Degussa alumina with an acetone solution of hexachloroplatinic acid (H_2PtCl_6) and $SnCl_4$ by incipient wetness technique. CAT-B was prepared by a coprecipitation technique (*26*), in which the required amounts of $SnCl_4 \cdot 5H_2O$ and aluminum nitrate were dissolved in water. This solution was heated to 60°C and ammonium hydroxide was added to effect precipitation at pH 7–8. The hydrous gel was heated at 60°C for 6 h maintaining the pH at 7–8. The gel was recovered by filtration and the precipitate was washed and then dried at 120°C overnight. The oxide gel was then pulverized and calcined at 500°C for 6 h, and the required amount of hexachloroplatinic acid was impregnated on the support. In both catalysts the Pt to Sn mole ratio was Pt : Sn = 1 : 3. After impregnation with an acetone solution of the Pt and Sn compounds these catalysts were dried at 120°C overnight. BET surface areas (*27*) were calculated from nitrogen adsorption isotherms using a quantachrome autosorb instrument. Prior to analysis, the samples were outgassed at 150°C overnight and approximately at 10 mTorr. The surface areas of CAT-A and CAT-B were 110 m^2/g and 180 m^2/g, respectively.

B. Reduction Treatment of Catalysts

About 2 g of catalyst powders were reduced in a glass reactor in flowing H_2 at 500°C for about 18 h. After reduction, the samples were cooled down to room temperature in H_2 flow and then passivated in a 1% O_2 in helium gas flow for 25 h. These passivated samples were utilized for XRD and TEM analyses. Earlier studies have shown that passivated samples provide XRD data that cannot be distinguished from

that obtained by an *in situ* instrument (*28, 29*).

C. X-Ray Diffraction

In order to obtain structural information, the passivated catalysts were analyzed in a Rigaku X-ray diffractometer using Cu$K\alpha$ radiation at 40 kV and 20 mA. This instrument was outfitted with an oriented pyrolytic graphite monochromator in the diffracted beam path. This unit is automated and a PDP 11/23 computer is interfaced to it. The 2θ step width was 0.02° with a counting time of 10 s at each step.

D. Electron Microdiffraction

TEM micrographs and data were obtained using a Hitachi H800 NA microscope. The operating voltage was 200 kV. The TEM samples were prepared by suspending the particles of the passivated catalyst samples in absolute ethanol. An optimum ratio of alcohol to powder particles was determined so that the particles are suspended to form a slightly turbid suspension. This suspension was constantly agitated in an ultrasonic bath. A drop of the suspension was carefully placed with a syringe on a carbon-coated copper grid. The alcohol evaporated leaving the fine particles on the grid, and the specimen was then loaded into the microscope for analysis.

RESULTS AND DISCUSSION

The X-ray diffraction patterns obtained for the reduced catalysts are shown in Fig. 1. The alloy phase PtSn (hcp) is identified for the PtSn/Degussa Al_2O_3 (Fig. 1a); however, this phase cannot be readily detected in the XRD trace for the coprecipitated catalyst (Fig. 1b). Difficulties have been encountered consistently in detecting the alloy phases on high surface area alumina support using XRD. However, for increased amounts of tin loadings with constant Pt, this alloy phase can be identified even on high surface area alumina support (*29*). The inability to identify alloy phases by XRD may be due to a high dispersion of fine metallic particles on the support. A large molar excess of tin appears to result in the formation of alloy by a higher fraction of the Pt so that an alloy phase can be identified by XRD (*29*).

Using 2- and 5-nm electron probes, electron microdiffraction data were collected from both samples CAT-A and CAT-B. Figure 2 shows a micrograph of catalyst particles from CAT-A and Fig. 3 is the micrograph obtained from CAT-B. The metal particle size distributions obtained from these figures for the catalysts (Fig. 4) indicate that the Pt is better dispersed on the coprecipitated support. The particle size distribution peaks at ca. 6 nm for CAT-A and at ca. 4 for CAT-B (Fig. 4).

Microdiffraction patterns were obtained from particles of 2–10 nm in diameter. The observed diffraction patterns were compared with the patterns calculated using the lattice constants for various alloy phases shown in Table 1. A typical electron diffraction pattern from a particle is shown in Fig. 5(a) and the solution in Fig. 5(b). The pattern shows that the particle has PtSn (hcp) alloy structure aligned parallel to $[10\bar{1}2]$ zone axis. Note that the points in the reciprocal lattice which are forbidden on the basis of kinematic diffraction theory, appear in the observed pattern due to double diffraction effects.

A few diffraction patterns corresponded to the $PtSn_2$ (fcc) phase, although most of the patterns showed (PtSn) hcp structure. A typical diffraction pattern from a $PtSn_2$ (fcc)

TABLE 1

Crystallographic Information of the Pt–Sn Crystal Systems

Formula	Crystal structure	Lattice constants			Space group
		a	*b*	*c*	
PtSn	hcp (NiAs type)	4.100		5.432	$P6_3/mmc$
$PtSn_2$	fcc (CaF_2 type)	6.425			Fm3m
$PtSn_4$	Orthorhombic	6.362	6.393	11.311	C_{2v}–ABA2
Pt_2Sn_3	hcp	4.337		12.960	$P6_3/mmc$
Pt_3Sn	fcc (Cu_3Au type)	4.0005			—

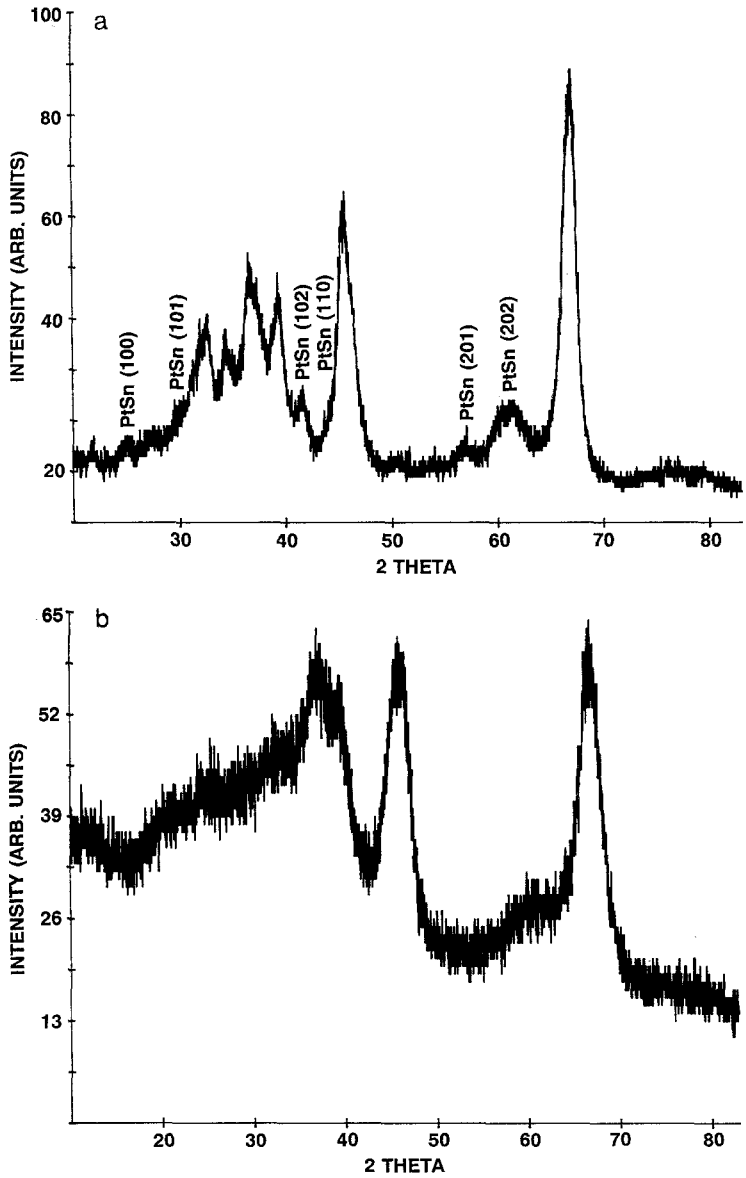

FIG. 1. (a) X-ray diffraction pattern obtained from the reduced and passivated catalyst CAT-A. The low-intensity peaks of PtSn (hcp) phase are present. (b) X-ray diffraction pattern obtained from the reduced and passivated catalyst CAT-B. The peaks due to PtSn (hcp) or to any other alloy phases cannot be observed.

particle is shown in Fig. 6, which is aligned parallel to [110] zone axis. This indicates that some of the excess of tin may combine with Pt to form alloys other than PtSn. These other alloy forms, however, could not be identified in XRD, due to their small crystallite sizes and/or to the much lower concentrations.

Electron microdiffraction studies reveal that Pt combines with tin to form at least two forms of Pt–Sn alloys, which are PtSn (close-packed hexagonal structure with

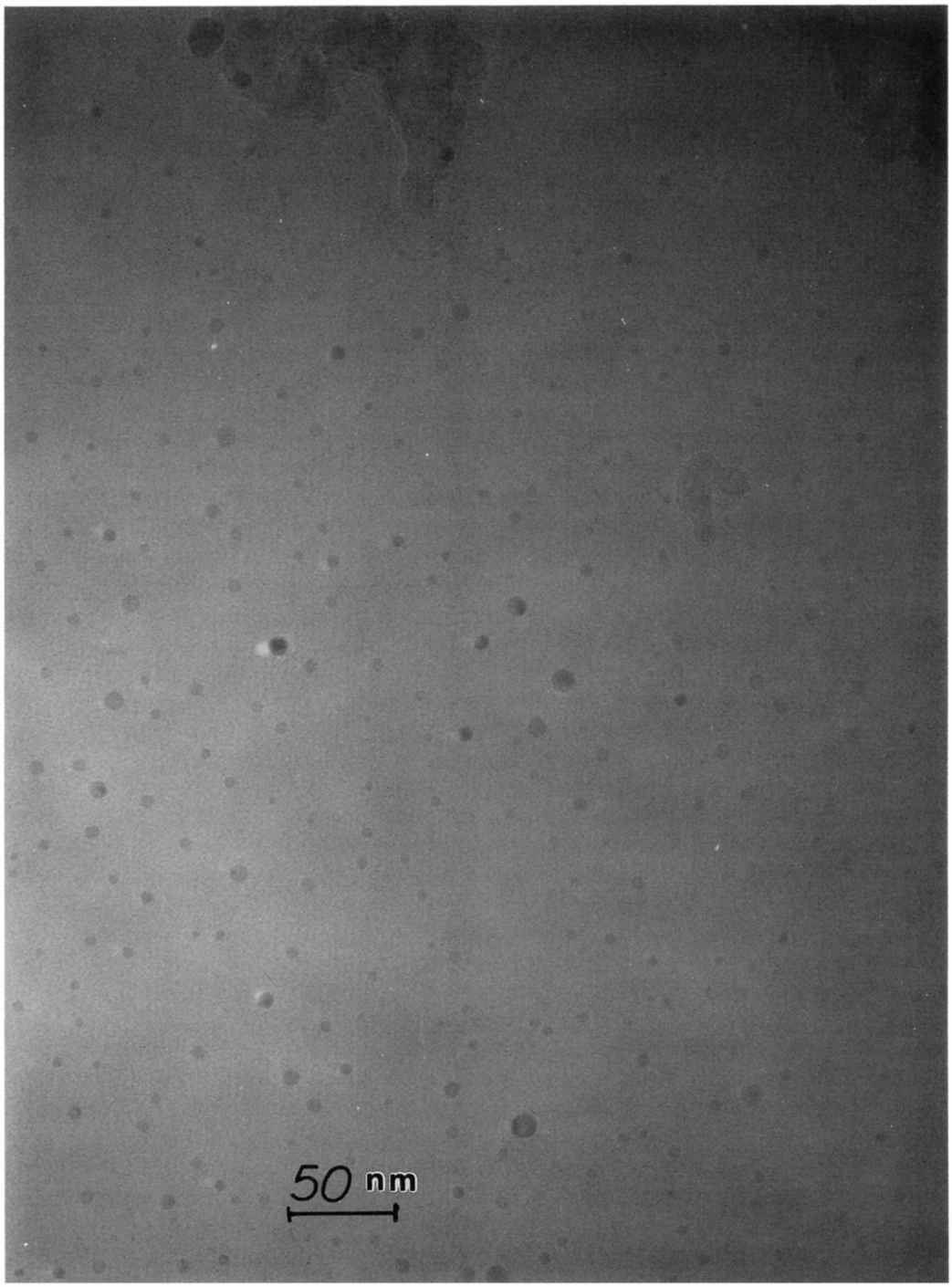

FIG. 2. Electron micrograph from CAT-A.

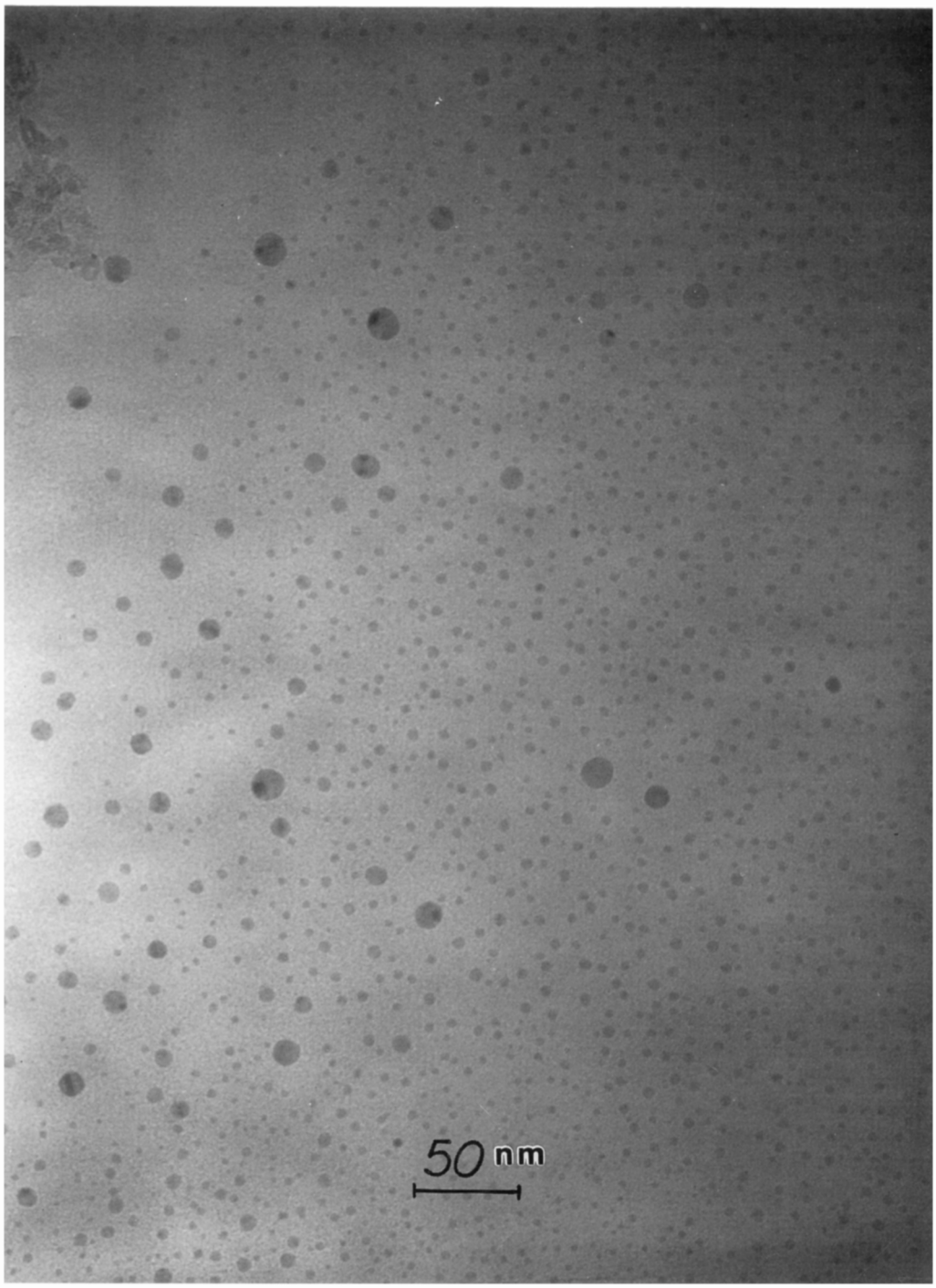

FIG. 3. Electron micrograph from CAT-B.

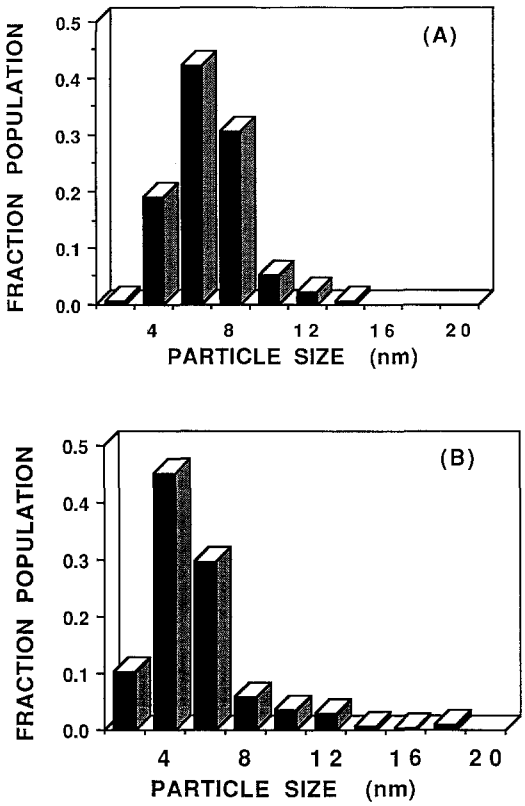

FIG. 4. Metal particle size distribution for CAT-A (A) and for CAT-B (B).

Pt : Sn = 1 : 1) and $PtSn_2$ (a CaF_2-type fcc structure). However, *in situ* X-ray diffraction study revealed the presence of only the Pt–Sn (hcp) alloy phase (*25, 28*). It was assumed that the excess tin must be present either in a metallic state or in the form of tin-aluminate. The microdiffraction study revealed that most of the particles possess PtSn (hcp) symmetry, while a few of them exhibit $PtSn_2$ (fcc) symmetry. Direct evidence is obtained for the presence of another form of alloy, i.e., $PtSn_2$, for these supported catalysts wherein it can be argued that a minor amount of the excess tin combines with Pt to form alloys other than Pt : Sn = 1 : 1. Microdiffraction studies combined with EDX measurements of the amounts of tin alloyed with Pt have been carried out and are described below.

EDX measurements were undertaken in an attempt to identify the extent of formation of alloys other than the PtSn alloy identified by XRD. For CAT-B many catalyst particles could be examined without detecting Pt–Sn alloys even when Pt peaks could be clearly discerned (Fig. 7). The intensity versus energy scans obtained for four particles are shown in Fig. 7. All four scans are for the same energy range. The $PtL\alpha_1$ peak, identified in the lower left scan, is presented as a heavier line in the four scans. As the $PtL\alpha_1$ peak intensity varies in the four scans, the presence of Pt is confirmed. The location for the $SnL\alpha_1$ peak is indicated in the lower left scan; however, there is no evidence for the Sn peak in these four scans. Thus, the Pt/Sn alloy detected in a few particles in the microdiffraction studies does not appear to be representative of the major fraction of the Pt present in the sample. Also, since the atomic ratio of Pt : Sn is 1 : 3 in the catalyst, it appears surprising at first that Pt can be detected but that Sn is not detected. However, EDX analysis is limited to that volume of sample exposed to the beam that lies within 10–100 nm of the surface for most heavy elements. Thus, it appears that the Pt added by impregnation is located on the surface of the support so that sufficient Pt is present in the sampled volume to be detected. The tin in this catalyst was added during coprecipitation and should be uniformly dispersed through the solid so that its concentration in the fraction of the volume sampled by EDX is low relative to that of Pt. This is an observation that has significant implications. Commercial formulations appear to be based upon coprecipitated catalysts. Thus, the catalyst improvement imparted by the incorporation of Sn does not appear to be related to Pt/Sn alloy formation.

Examination of a number of CAT-A particles with EDX shows that both Pt and Sn are observed (Fig. 8). As in Fig. 7, EDX intensity versus energy scans for four particles in CAT-A are shown in Fig. 8. The energy locations where the $SnL\alpha_1$ and $PtL\alpha_1$

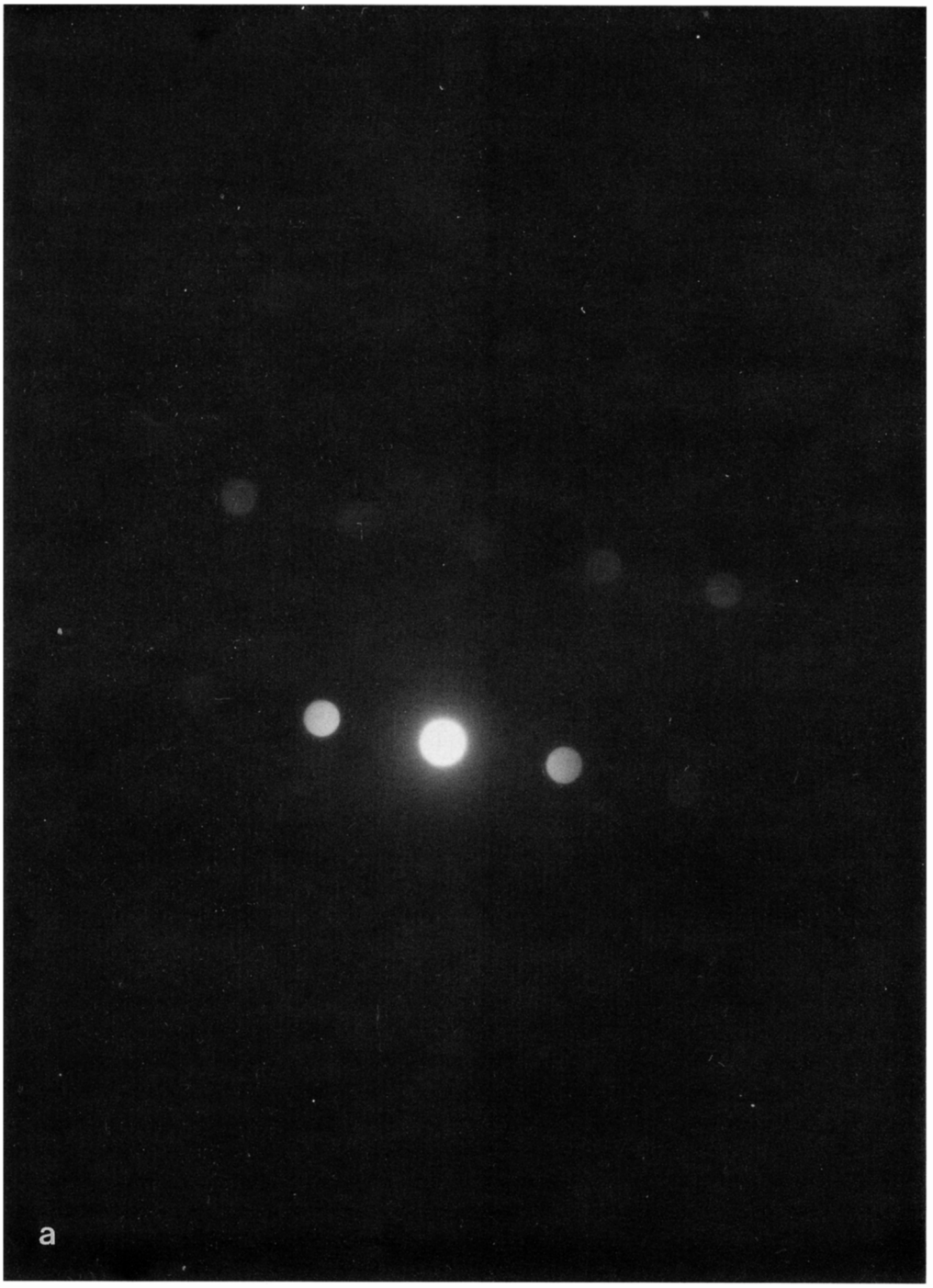

FIG. 5. (a) Electron microdiffraction pattern using a 5-nm electron probe from a PtSn (hcp) particle in CAT-B. (b) The solution for the observed pattern shown above. (△) observed reflections, (○) calculated reflections, and (X) forbidden reflections, which appear due to double diffraction.

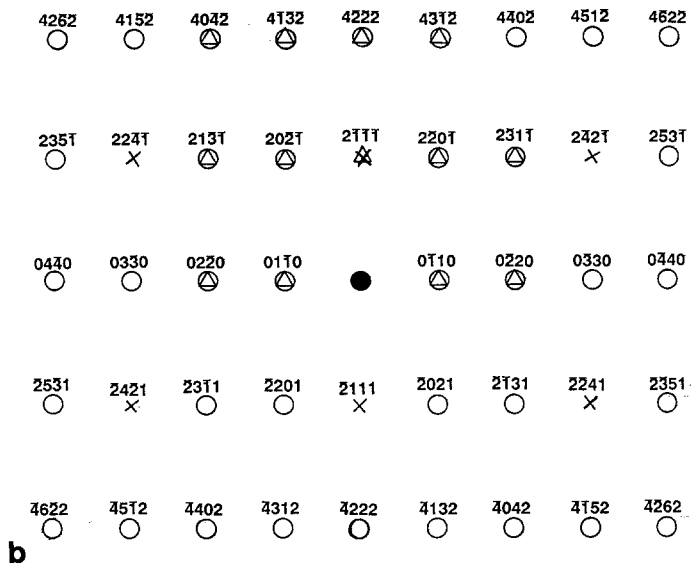

FIG. 5—*Continued*

peaks are expected to occur are indicated in the lower left scan. The peaks corresponding to these two energies, indicated by the heavily darkened peaks, are present in all four scans. This catalyst differs from CAT-B in two respects: (1) the alumina is an agglomeration of nonporous spheres and (2) both Pt and Sn were added by coimpregnation. Thus, in CAT-A, both Pt and Sn are expected to be present on the external surface of alumina spheres. EDX analysis of ca. 25 catalyst particles provide a range of Sn/Pt ratios; however, plotting the number of particles of a particular Sn/Pt range versus increasing ranges of Sn/Pt produces a distribution that is dominated by peaks consistent with Pt : Sn alloy = 1 : 1 (Fig. 9). Thus, the EDX data for CAT-A leads to the same conclusion as XRD data for this catalyst: the dominant alloy form of Pt is Pt : Sn = 1 : 1.

CAT-A is prepared by an incipient wetness technique to contain Pt : Sn = 1 : 3; however, the EDX data indicate a Pt : Sn ratio of 1 : 1. This indicates that a significant fraction of the Sn is not detected by EDX. The EDX data are consistent with a material where Pt and Sn agglomerate so that sufficient Pt and Sn are present in the analyzed area to permit both Pt and Sn to be detected, and the average Pt/Sn ratio in these agglomerates is 1. With the Degussa alumina support, it appears unlikely that Sn, added to the surface by incipient wetness impregnation, would migrate to the bulk of the alumina during heating at 500°C. Thus, the EDX data are consistent with a fraction of the Sn being concentrated in PtSn alloy and the remaining fraction (at least two-thirds of the added Sn) is distributed over the surface of Degussa alumina. Using the crystallographic data for SnO_2, one can obtain a geometrical area occupied by a surface SnO_2 grouping. For nonporous alumina with an area of 110 m^2/g, at least 6 wt% Sn is required to provide a surface monolayer of tin oxide. Thus, if all Pt is present as Pt : Sn = 1 : 1, the remaining Sn in CAT-A would be sufficient to provide only ca. 0.2 of a monolayer. Thus, the EDX data for CAT-A are consistent with a model advanced for this catalyst based upon XPS (*8, 18, 19*) and XRD data (*25, 28, 29*): the surface of the alumina consists in part of surface monolayer of a tin aluminate compound and the other part is present as a Pt : Sn = 1 : 1 alloy.

Handy *et al.* examined the morphology of

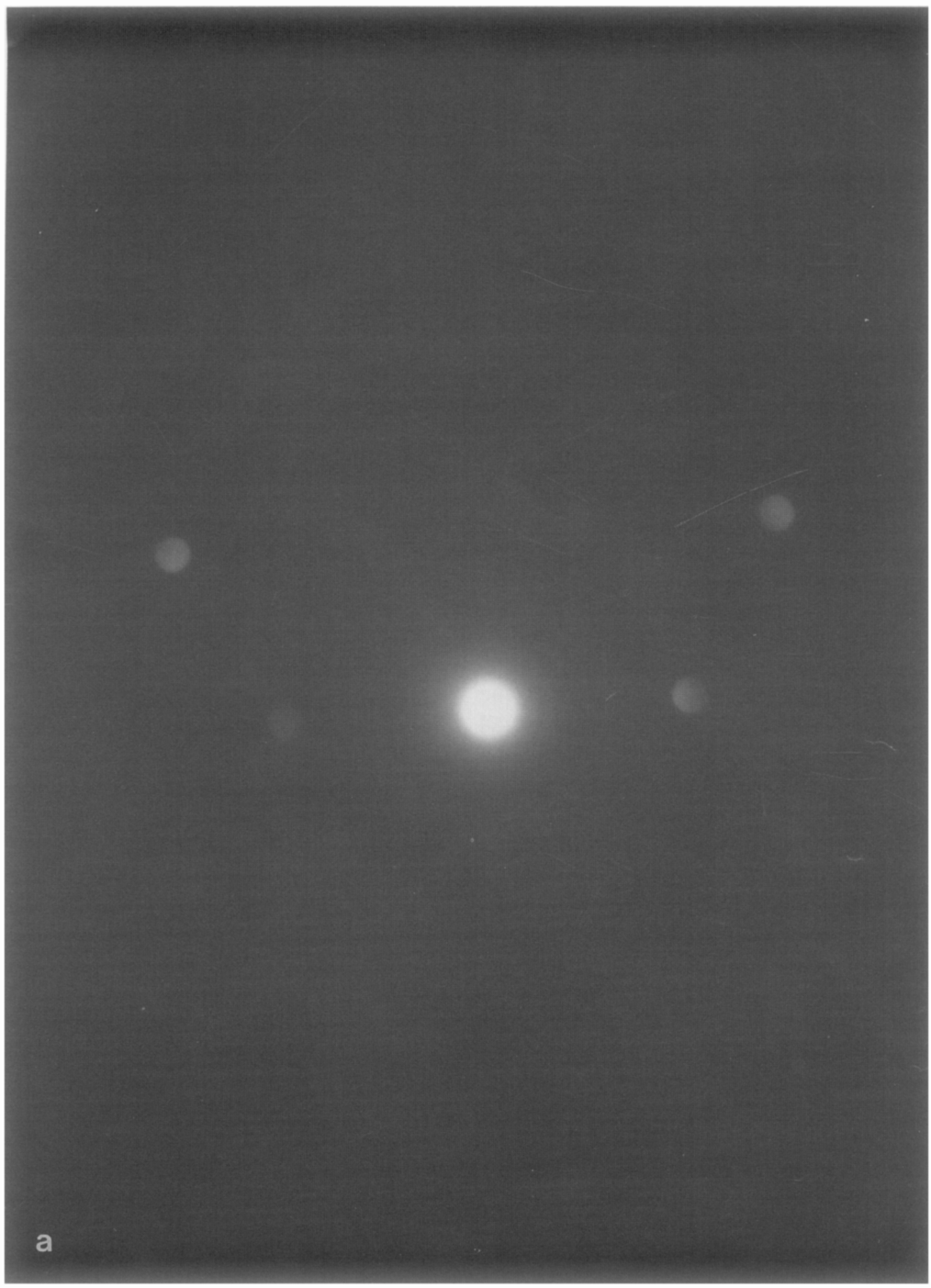

FIG. 6. (a) Electron microdiffraction pattern from an fcc ($PtSn_2$) particle of CAT-B, aligned parallel to [110] zone axis, and (b) the solution for the observed pattern. (△) observed reflections, (○) calculated reflections.

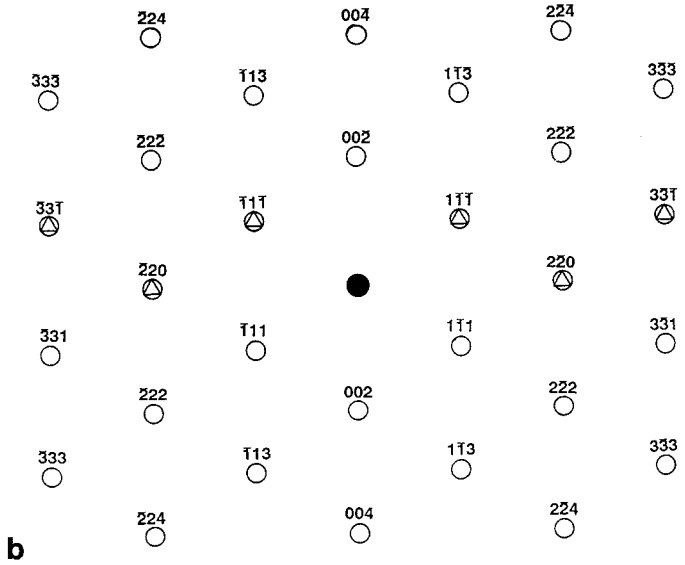

FIG. 6—*Continued*

Pt–Sn phases on thin films of alumina (*30*). They reported that the composition of the alloy formed varied with the relative amounts of metal deposited by evaporation onto the alumina film. They observed a Pt–Sn alloy of 0.5 : 1 and 1 : 1 composition. Paffett and Windham (*31*) reported that Pt rich alloys are formed on Pt(111) by Sn adatoms upon annealing at 727°C. The present results indicate that the $PtSn_2$ phase, as well as alloy phases other than PtSn, are of minor importance in catalysts supported on high area alumina.

Tin alters the activity and aromatic selectivity of a Pt catalyst, which implies an intimate contact between some form of tin and Pt(O). Catalytic activity appears to go through a maximum near Sn/Pt ~3 to 4 (*32*) for activity for dehydrocyclization at 1 atm. CAT-A appears, under similar reaction conditions, to be much more resistant to aging during *n*-octane conversion at 1 or 10 atm

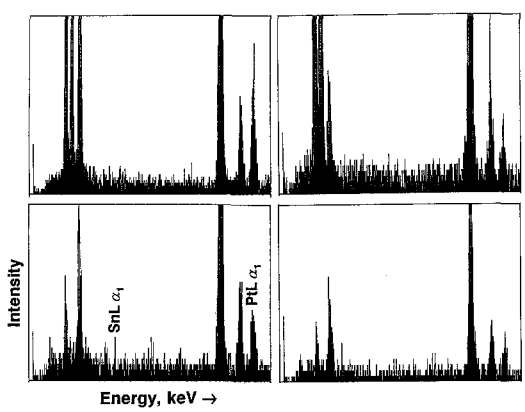

FIG. 7. Representative EDX traces for four CAT-B particles.

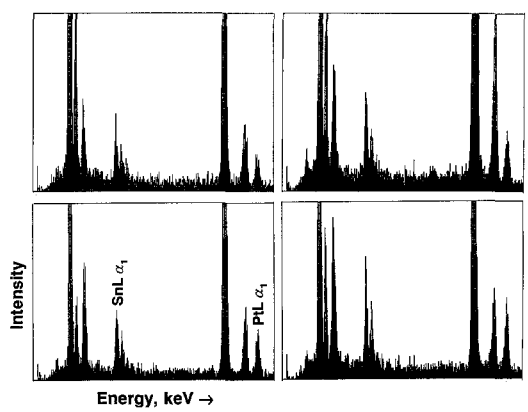

FIG. 8. Representative EDX traces for four CAT-A particles.

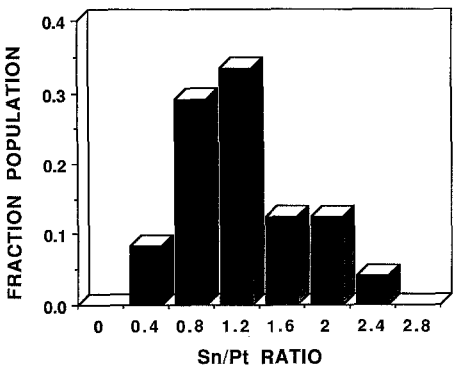

FIG. 9. Frequency distribution of EDX intensity of Sn/Pt ratios for increasing Sn/Pt concentration.

pressure (*29*) but the Sn/Pt ratio for maximum activity varies with total pressure. These observations raise a question about the identity of the catalytically active species in the PtSn alumina catalyst: Is it the PtSn alloy or is it X-ray amorphous Pt that is modified to become more active by contact with a Sn species? Activity as used here must include a factor that takes into consideration the aging resistance since it may be the ability of Sn to retard aging that provides an apparent increase in activity. If the maximum in activity at a Sn–Pt ratio of 3 to 4 is valid then the implication is that it is the dispersed, X-ray-amorphous Pt, rather than the PtSn (1 : 1) alloy, that is catalytically active for hydrocarbon conversions.

REFERENCES

1. Jacobson, R. L., Kluksdahl, H. E., McCoy, C. S., and Davis, R. W., *Proc. Amer. Petrol. Inst. Div.* **49,** 504 (1969).
2. Beeck, O., *Discuss. Faraday Soc.* **8,** 118 (1950).
3. McNicol, B. D., *J. Catal.* **46,** 438 (1977).
4. Kuznetsov, V. I., Yurchenlca, E. N., Belyi, A. S., Zatolokina, E. V., Smolikov, M. A., and Duplakin, V. K., *React. Kinet. Catal. Lett.* **21,** 419 (1982).
5. Bacaud, R., Bussiere, P., and Figueras, F., *J. Catal.* **69,** 399 (1981).
6. Burch, R., *J. Catal.* **71,** 348 (1981).
7. Short, D. R., Khalid, S. M., Katzer, J. R., and Kelley, M. J., *J. Catal.* **72,** 288 (1981).
8. Adkins, S. R., and Davis, B. H., *J. Catal.* **89,** 371 (1984).
9. Davis, B. H., *J. Catal.* **46,** 348 (1977).
10. Sinfelt, J. H., "Bimetallic Catalysis: Discoveries, Concepts, and Applications." Wiley, New York, 1983.
11. Bolivar, G., Charcosset, M., Ferty, R., Primet, M., and Tournayan, L., *J. Catal.* **37,** 424 (1975).
12. Wagstaff, N., and Prins, R., *J. Catal.* **59,** 434 (1979).
13. Burch, R., *Platinum Metals Rev.* **22,** 57 (1978).
14. Sexton, B. A., Hughes, A. E., and Foger, K., *J. Catal.* **88,** 466 (1984).
15. Kuznetsov, V. I., Belyi, A. S., Yurchenko, E. N., Smolikov, M. D., Protasova, M. T., Zatolokina, E. V., and Duplyakin, V. K., *J. Catal.* **99,** 159 (1986).
16. Müller, A. C., Engelhard, P. A., and Weisang, J. E., *J. Catal.* **56,** 65 (1979).
17. Lieske, H., and Volter, J., *J. Catal.* **90,** 46 (1984).
18. Li, Y.-X., Stencel, J. M., and Davis, B. H., *Reaction Kin. Catal. Lett.* **37,** 273 (1988).
19. Li, Y.-X., Stencel, J. M., and Davis, B. H., *Appl. Catal.,* **64,** 71 (1990).
20. Adkins, S. R., and Davis, B. H., *in* "Catalyst Characterization Science" (M. L. Deviney and J. L. Gland, Eds.), ACS Symp. Series, Vol. 288, p. 57. Am. Chem. Soc., Washington, DC, 1985.
21. Zhang, S., Xie, B., Wang, P., and Zhang, J., *Ts' Us Hua Hseuh Pao,* **1** (4), 253 (1980).
22. Li, Y. X., Zhang, Y. F., and Shia, Y. F., *J. Catal. (China),* **5,** 311 (1985).
23. Hansen, M., "Constitution of Binary Alloys," McGraw-Hill, New York, 1958, pg. 1142.
24. Ushakov, V. A., and Moroz, E. M., *React. Kinet. Catal. Lett.,* **27,** 351 (1985).
25. Srinivasan, R., De Angelis, R. J., and Davis, B. H., *J. Catal.,* **106,** 449–457 (1987).
26. Meitzner, G., Via, G. H., Lytle, F. W., Fung, S. C., and Sinfelt, J. H., *J. Phys. Chem.,* **92,** 2925 (1988).
27. Brunauer, S., Emmett, P. H., and Teller, E., *J. Am. Chem. Soc.,* **60,** 309 (1938).
28. Srinivasan, R., De Angelis, R. J., and Davis, B. H., *Catalysis Letters,* **4,** 303 (1990).
29. Srinivasan, R. and Davis, B. H., unpublished data.
30. Handy, B. E., Dumesic, J. A., Sherwood, R. D., and Baker, R. T. K., *J. Catal.,* **24,** 160 (1990).
31. Paffett, M. T., and Windham, R. G., *Surf. Sci.,* **208,** 34 (1989).
32. Davis, B. H., Bimetallic Catalyst Preparation, U.S. Patent 3,840,475, October 8, 1974.